

Pathogenesis of A⁻β⁺ Ketosis-Prone Diabetes

Sanjeet G. Patel,¹ Jean W. Hsu,² Farook Jahoor,² Ivonne Coraza,¹ James R. Bain,^{3,4} Robert D. Stevens,^{3,4} Dinakar Iyer,¹ Ramaswami Nalini,^{1,5} Kerem Ozer,^{1,5} Christiane S. Hampe,⁶ Christopher B. Newgard,^{3,4} and Ashok Balasubramanyam^{1,5}

A⁻β⁺ ketosis-prone diabetes (KPD) is an emerging syndrome of obesity, unprovoked ketoacidosis, reversible β-cell dysfunction, and near-normoglycemic remission. We combined metabolomics with targeted kinetic measurements to investigate its pathophysiology. Fasting plasma fatty acids, acylcarnitines, and amino acids were quantified in 20 KPD patients compared with 19 nondiabetic control subjects. Unique signatures in KPD—higher glutamate but lower glutamine and citrulline concentrations, increased β-hydroxybutyryl-carnitine, decreased isovaleryl-carnitine (a leucine catabolite), and decreased tricarboxylic acid (TCA) cycle intermediates—generated hypotheses that were tested through stable isotope/mass spectrometry protocols in nine new-onset, stable KPD patients compared with seven nondiabetic control subjects. Free fatty acid flux and acetyl CoA flux and oxidation were similar, but KPD had slower acetyl CoA conversion to β-hydroxybutyrate; higher fasting β-hydroxybutyrate concentration; slower β-hydroxybutyrate oxidation; faster leucine oxidative decarboxylation; accelerated glutamine conversion to glutamate without increase in glutamate carbon oxidation; and slower citrulline flux, with diminished glutamine amide-nitrogen transfer to citrulline. The confluence of metabolomic and kinetic data indicate a distinctive pathogenic sequence: impaired ketone oxidation and fatty acid utilization for energy, leading to accelerated leucine catabolism and transamination of α-ketoglutarate to glutamate, with impaired TCA anaplerosis of glutamate carbon. They highlight a novel process of defective energy production and ketosis in A⁻β⁺ KPD. *Diabetes* 62:912–922, 2013

Ketosis-prone diabetes (KPD) is characterized by presentation with diabetic ketoacidosis (DKA) in persons who do not fit traditional categories of types 1 or 2 diabetes (1–5). We have defined four subgroups of KPD based on presence or absence of β-cell autoantibodies (A⁺ or A⁻), and recovery or lack of recovery of β-cell functional reserve following the index episode of DKA (β⁺ or β⁻) (1,6,7).

From the ¹Translational Metabolism Unit, Diabetes/Endocrinology Research Center, Baylor College of Medicine, Houston, Texas; the ²Department of Pediatrics, Children's Nutrition Research Center, Baylor College of Medicine, Houston, Texas; the ³Sarah W. Stedman Nutrition and Metabolism Center, Duke University Medical Center, Durham, North Carolina; the ⁴Department of Pharmacology and Cancer Biology, Duke University Medical Center, Durham, North Carolina; the ⁵Endocrine Service, Ben Taub General Hospital, Houston, Texas; and the ⁶Department of Medicine, University of Washington, Seattle, Washington.

Corresponding author: Ashok Balasubramanyam, ashokb@bcm.edu.

Received 17 May 2012 and accepted 19 August 2012.

DOI: 10.2337/db12-0624

S.G.P. and J.W.H. are joint first authors.

S.G.P. is currently affiliated with the Department of Surgery, UCLA Medical Center, Los Angeles, California.

© 2013 by the American Diabetes Association. Readers may use this article as long as the work is properly cited, the use is educational and not for profit, and the work is not altered. See <http://creativecommons.org/licenses/by-nc-nd/3.0/> for details.

See accompanying commentary, p. 682.

The A⁻β⁺ KPD subgroup represents a novel syndrome of severe but reversible β-cell dysfunction (1,3,5,8,9). Approximately 50% of these patients develop DKA without a precipitating factor at diagnosis of diabetes. These new-onset, unprovoked A⁻β⁺ KPD patients display male predominance (10) and low frequencies of human leukocyte antigen class II susceptibility alleles for autoimmune diabetes (11). β-Cell function increases markedly within 1–3 months after the index DKA, with sustained glycemic improvement and insulin independence (1,9,11,12). The cause of the unprovoked ketoacidosis is unknown. Over 5–10 years, patients may relapse to unprovoked ketosis (3,5).

This syndrome provides a model to identify novel mechanisms of obesity, ketosis, and reversible β-cell dysfunction. We used a metabolomics approach to identify unique alterations in A⁻β⁺ KPD patients, with a kinetics approach to specify the pathophysiology.

RESEARCH DESIGN AND METHODS

Metabolomic analysis

Human subjects. Protocols were approved by the Human Studies Institutional Review Boards of Baylor College of Medicine and Duke University (13). Written informed consent was obtained. New-onset, unprovoked male A⁻β⁺ KPD patients ($n = 20$) were identified by absence of GAD65/67, IA-2, or ZnT8 autoantibodies and presence of β-cell functional reserve 4–8 weeks after the index DKA (1,6). Men ($n = 19$) from the Study of the Effects of Diet on Metabolism and Nutrition study (13) were nondiabetic obese control subjects. KPD patients were selected from a longitudinal database using the MatchIT program (15) to minimize intragroup differences in initial HbA_{1c} and intergroup differences in age, ethnicity, BMI, waist circumference, fasting C-peptide, glucose, and lipids. At the time of blood sampling, all patients were clinically stable, taking twice-daily neutral protamine Hagedorn insulin (\pm short-acting insulin); three patients were also taking metformin (1 g daily). Five additional, newly diagnosed, unprovoked A⁻β⁺ KPD patients were subsequently recruited for measurements of glutamine, glutamate, isoleucine, and leucine.

Plasma collection. The KPD samples were collected in acid citrate dextrose (#364606, BD Biosciences) after an overnight fast before the morning dose of insulin, 20 days (median) after the index DKA (5). Blood was kept on ice for 2–4 h, centrifuged at 4°C, and the plasma stored at -20°C. Control subjects' samples were collected after an overnight fast in serum separator tubes (#366510, BD Biosciences), centrifuged, and the serum stored at -80°C. Blood samples were also taken from five fresh A⁻β⁺ KPD patients 1 month after their index DKA, collected in serum separator tubes, processed immediately, and stored.

Metabolite analysis. To measure 15 amino acids and 45 acylcarnitines, samples were deproteinized by methanol precipitation, esterified with hot, acidic methanol or *n*-butanol, and then analyzed by tandem mass spectrometry (MS/MS) with a Quattro Micro instrument (Waters Corporation, Milford, MA) (13). Leucine and isoleucine are reported as a single analyte (Leu/Ile) because they were not resolved by this method. These conditions partially hydrolyze glutamine to glutamate and asparagine to aspartate, so “glx” (Glu/Gln) or “asx” (Asp/Asn) signify glutamate or aspartate with contributions from hydrolysis reactions of glutamine and asparagine. Final concentrations of isoleucine, leucine, glutamine, and glutamate were measured by reverse-phase high-performance liquid chromatography (HPLC; Hewlett-Packard 1090; Hewlett-Packard, Avondale, PA); frozen samples were thawed on ice prior to HPLC and glutamine standards prepared fresh in ice-cold water.

To measure seven nonesterified free fatty acids (FFAs), samples were methylated and purified by solid-phase extraction (13). Derivatized fatty acids

were analyzed by gas chromatography/mass spectrometry (GC/MS; Trace DSQ; Thermo Electron Corporation, Austin, TX).

All MS analyses used stable isotope dilution to quantify metabolites (13). Because acid citrate dextrose tubes were used for the original KPD patients, a dilution correction factor (1.31) was used for analytes measured in those samples (16).

Plasma insulin, C-peptide, glucagon, cortisol, and free metanephrines were measured by radioimmunoassay (Linco, St. Louis, MO), and β -hydroxybutyrate (BOHB) by spectrophotometry (Wako, Richmond, VA).

Statistical analysis. Data were inspected for normality using the Shapiro-Wilk tests. The *t* tests were used to compare levels of hormones, baseline clinical parameters, and metabolites. BOHB values were not normally distributed, so median levels were compared using the Mann-Whitney U test. The Fisher exact test was used to assess deviations from the order of metabolites as an indicator of substrate preference due to altered consumption or production. Significance was defined at $P < 0.05$.

Kinetic analyses

Human subjects. The study was approved by the Baylor institutional review board and written informed consent obtained. Nine new-onset, unprovoked $A^{-}\beta^{+}$ KPD patients (six men, three women), all clinically stable, were recruited 6–8 weeks after the index DKA episode. Seven nondiabetic control subjects (six men, one woman) were matched for BMI, age, and ethnicity, with the six men and one woman among the KPD patients. Exclusions were: serum creatinine >1.2 mg/day, retinopathy, neuropathy, or heart failure; history of alcohol abuse; alanine aminotransferase/aspartate aminotransferase (AST)/alkaline phosphatase $>2\times$ upper limit of normal; medications likely to affect fat, glucose, or protein metabolism; and other chronic illnesses. Fasting plasma C-peptide and glucose, peak and area under the curve of C-peptide response to glucagon, fasting lipids, and liver and thyroid functions were measured. Details of the glucagon stimulation test and cutoffs to classify β -cell reserve have been reported (1).

Subjects underwent four stable isotope protocols in the General Clinical Research Center. For 2 days prior to each study, they consumed an isocaloric, standardized diet (30% calories from fat, 65% from carbohydrates, 1 g/kg protein) prepared by the General Clinical Research Center kitchen. KPD patients were treated with low doses of neutral protamine Hagedorn insulin for 8 weeks prior to the studies. The last dose was administered at 8–10 P.M., and each study commenced the following morning after a 10–14-h fast, with no insulin administered until study completion. One venous catheter was placed for infusions, with another in the opposite hand, heated for arterialized blood sampling.

Protocol 1. After baseline blood and breath sampling, an oral 50 mg/kg bolus of $^2\text{H}_2\text{O}$ was administered. After an intravenous priming dose of $\text{NaH}^{13}\text{CO}_3$ (1.2 $\mu\text{mol/kg}$), $^2\text{H}_5$ -glycerol (prime 4.5 $\mu\text{mol/kg}$, constant 9.0 $\mu\text{mol/kg/h}$), $^2\text{H}_2$ -potassium palmitate (prime 3 $\mu\text{mol/kg}$, constant 4 $\mu\text{mol/kg/h}$), and $^{13}\text{C}_1$ -acetate (prime 62.5 $\mu\text{mol/kg}$, constant 150 $\mu\text{mol/kg/h}$) were infused for 4 h. Blood was collected hourly for the first 3 h and every 15 min during the fourth hour. Indirect calorimetry was performed during the last 30 min of the fourth hour. At hour 4, glycerol and palmitate infusions ceased, but the acetate infusion continued for another 2 h. Blood and breath samples were drawn every 15 min between hours 5 and 6.

Tracer-to-tracee ratios of plasma free palmitate, acetate, and BOHB were determined by negative chemical ionization GC/MS of its pentafluorobenzyl derivative (17). Plasma palmitate and BOHB concentrations were measured by in vitro isotope dilution with $\text{U-}^{13}\text{C}$ -palmitate or $^{13}\text{C}_2$ -BOHB (Cambridge Isotope Laboratories, Andover, MA) as internal standards, using negative chemical ionization-GC/MS (17).

Tracer-to-tracee ratio of plasma glycerol was determined by electron impact ionization GC/MS of its tripropionate derivative (18). Breath $^{13}\text{CO}_2$ content was determined by GC/gas isotope ratio MS. Zinc was used to reduce water in 10- μl plasma in quartz vessels and $^2\text{H}_2$ abundance of the resulting hydrogen determined by GC/gas isotope ratio MS.

Protocol 2. After baseline blood sampling, $^2\text{H}_2$ -citrulline (prime 1.0 $\mu\text{mol/kg}$, constant 1.0 $\mu\text{mol/kg/h}$), $^{15}\text{N}_1$ -amide-glutamine (prime 13.6 $\mu\text{mol/kg}$, constant 13.6 $\mu\text{mol/kg/h}$), $^2\text{H}_5$ -valine (prime 1 $\mu\text{mol/kg}$, constant 1 $\mu\text{mol/kg/h}$), and $\text{NaH}^{13}\text{CO}_3$ (prime 4 $\mu\text{mol/kg}$, constant 4 $\mu\text{mol/kg/h}$) were infused. A 0.5- $\mu\text{mol/kg}$ prime of $^{15}\text{N}_1$ -citrulline was also given. Citrulline, glutamine, and valine were infused for 6 h. $\text{NaH}^{13}\text{CO}_3$ infusion was infused for 2 h; at the second hour, $^{13}\text{C}_1$ -leucine (prime 4 $\mu\text{mol/kg}$, constant 4 $\mu\text{mol/kg/h}$) was started and infused until hour 6. Blood was collected hourly during the first 4 h and every 15 min during the fifth hour. Breath was collected at baseline and every 15 min between hours 1 and 2 and 5 and 6.

Tracer-to-tracee ratio of plasma α -ketoisocaproic acid (α -KICA) from leucine was measured by negative chemical ionization-GC/MS of its pentafluorobenzyl derivative (17).

Plasma citrulline, glutamine, and valine isotopic enrichment (IE) were measured after conversion to their 5-(dimethylamino)-1-naphthalene sulfonamide

derivatives by liquid chromatography-MS/MS (Synergi MAX-RP column; Phenomenex, Torrance, CA) (19).

Protocol 3. After baseline blood and breath sampling, $^{13}\text{C}_1$ -glutamine (prime 13.6 $\mu\text{mol/kg}$, constant 13.6 $\mu\text{mol/kg/h}$) was infused for 6 h. A priming dose of $\text{NaH}^{13}\text{CO}_3$ (4 $\mu\text{mol/kg}$) was given at hour 0. Indirect calorimetry was performed during the last 30 min of the fourth hour. Blood and breath were collected hourly for 5 h and then every 15 min between hours 5 and 6.

Plasma glutamine and glutamate IE were measured by liquid chromatography-MS/MS as in protocol 2.

Protocol 4. After baseline blood and breath sampling, a priming dose of $\text{NaH}^{13}\text{CO}_3$ (4 $\mu\text{mol/kg}$) was given, and then 2,4- ^{13}C - β -hydroxybutyrate (prime 20 $\mu\text{mol/kg}$, constant 12 $\mu\text{mol/kg/h}$) was infused for 3 h. Blood and breath were collected hourly for the first 2 h and every 15 min during the third hour. Indirect calorimetry was performed during the last 30 min of the second hour. Blood was collected in K-EDTA tubes and spun immediately and one aliquot deproteinized with perchloric acid and frozen in liquid nitrogen.

IE of BOHB was measured as in protocol 1.

Plasma glucose was measured with a glucose analyzer (YSI, Yellow Springs, OH), insulin by radioimmunoassay (Linco) and FFAs by spectrophotometry (Wako). Amino acids were measured by HPLC.

Calculations. Ra (palmitate, glycerol, acetate, or BOHB) (in $\mu\text{mol/kg/h}$):

$$Ra(\mu\text{mol} \cdot \text{kg}^{-1} \cdot \text{h}^{-1}) = \left[\frac{IE_{\text{inf}}}{IE_{\text{p}}} - 1 \right] \times i, \quad \text{Eq. (1)}$$

where IE_{inf} is the IE (mole %) in the infusate, IE_{p} is IE (mole %) in the plasma at steady state, and i is the tracer infusion rate.

Rate of appearance of FFAs ($\mu\text{mol} \cdot \text{kg}^{-1} \cdot \text{h}^{-1}$):

$$Ra_{\text{FFA}} = \frac{Ra_{\text{palmitate}}}{\frac{[\text{palmitate}]_{\text{p}}}{[\text{FFA}]_{\text{p}}}}, \quad \text{Eq. (2)}$$

where Ra palmitate is the rate of appearance of palmitate (Eq. 1), $[\text{palmitate}]_{\text{p}}$ is the concentration of plasma palmitate, and $[\text{FFA}]_{\text{p}}$ is the concentration of plasma FFA.

Whole-body fatty acid oxidation is calculated from RQ, VO_2 , and $\dot{V}\text{CO}_2$ (20).

Rate of acetate oxidation ($\mu\text{mol} \cdot \text{kg}^{-1} \cdot \text{h}^{-1}$) in the tricarboxylic acid (TCA) cycle:

$$\text{Acetate}_{\text{OX}} = \left[\left(\dot{V}\text{CO}_2 / 0.56 \right) \times IE_{\text{CO}_2} \right] / (IE_{\text{acetate}}), \quad \text{Eq. (3)}$$

where $\dot{V}\text{CO}_2$ is the CO_2 excretion rate measured by indirect calorimetry, IE_{CO_2} is the IE of CO_2 in the breath, IE_{acetate} is the IE of plasma acetate, and 0.56 is the acetate retention factor (21).

Acetate oxidized in the TCA cycle (%):

$$\text{Percent}_{\text{oxidized}} = (\text{Acetate}_{\text{OX}} / Ra_{\text{acetate}}) \times 100, \quad \text{Eq. (4)}$$

BOHB from acetate ($\mu\text{mol/kg/h}$):

$$Q_{\text{acetate_BOHB}} = Ra_{\text{BOHB}} \times (IE_{\text{BOHB}}^{(M+1)} / IE_{\text{acetate}}), \quad \text{Eq. (5)}$$

where Ra_{BOHB} is the value from Eq. 1, $IE_{\text{BOHB}}^{(M+1)}$ is the M+1 isotopomer enrichment of BOHB derived from the $^{13}\text{C}_1$ -acetate infusate, and IE_{acetate} is the IE of acetate.

Total body water (TBW) (from oral deuterated water):

$$TBW(\text{ml}) = \frac{(E_{2\text{H}_2\text{O}} \times \text{Dose})}{(Ep_{2\text{H}_2\text{O}} \times 1.04)}, \quad \text{Eq. (6)}$$

where $E_{2\text{H}_2\text{O}}$ is the enrichment of deuterated water consumed, $Ep_{2\text{H}_2\text{O}}$ is the enrichment of plasma H_2O at steady state, and the constant 1.04 corrects for deuterium's volume of distribution. Fat-free mass (FFM) is $\text{TBW}/0.72$, where 0.72 is the hydration constant of fat-free tissue. Fat mass (kg) = body weight (kg) – FFM.

Ra (citrulline or glutamine amide-N) ($\mu\text{mol/kg/h}$) was calculated as in Eq. (1).

Rate of transfer of glutamine amide ^{15}N to citrulline:

$$Q_{\text{gh_cit}} = Ra_{\text{citrulline}} \times [IE_{\text{N-citrulline}}^{15} / IE_{\text{N-glutamine}}^{15}], \quad \text{Eq. (7)}$$

where Ra citrulline is the value from Eq. 7, $IE_{\text{N-citrulline}}^{15}$ is the isotopic (M+1) enrichment of citrulline from ^{15}N -glutamine, and $IE_{\text{N-glutamine}}^{15}$ is the isotopic (M+1) enrichment of glutamine.

Flux of glutamine carbon is calculated as in Eq. (7).

¹³C-glutamine reaches steady state quickly, but ¹³C-glutamate formed from the glutamine does not, because of the large whole-body free glutamate pool. Hence, the fraction of the glutamate pool derived from glutamine (fractional synthesis rate [FSR] of glutamate from glutamine) is calculated using the precursor-product equation:

$$\text{FSR (\%/h)} = \left[(\text{IEglu}_{t_6} - \text{IEglu}_{t_3}) / \text{IEglu}_{pt} \right] \times 100/3, \quad \text{Eq. (8)}$$

where $\text{IEglu}_{t_6} - \text{IEglu}_{t_3}$ is the increase in glutamate IE from 3–6 h of the infusion, and IEglu_{pt} is the plateau IE of glutamine.

TABLE 1
Metabolomic survey: demographic and biochemical data and fasting plasma concentrations of amino acids, acylcarnitines, and FFAs

	Control subjects (N = 19)	A ⁻ β ⁺ KPD (N = 20)	P value
Age (years)	50.7 ± 2.7	41.9 ± 2.1	0.02
BMI (kg/m ²)	33.8 ± 0.9	34.2 ± 1.5	0.8
Waist circumference (cm)	110.8 ± 1.4	114.5 ± 3.9	0.39
Initial ^A fasting glucose (mg/dL)	106 ± 3	241 ± 18	<0.001
Initial ^A fasting C-peptide (ng/mL)	3.53 ± 0.36	1.61 ± 0.25	<0.001
Initial ^A C-peptide/glucose	0.03 ± 0.001	0.01 ± 0.001	<0.001
Insulin (μU/mL)	27.9 ± 5.1	23.1 ± 6.0	0.55
QUICKI ^B	0.30 ± 0.01	0.29 ± 0.07	0.25
β-Hydroxybutyrate (μmol/L)	37.8 ± 4.5	74.1 ± 40.7	0.4
Total cholesterol (mg/dL)	194.2 ± 6.1	191.5 ± 10.8	0.8
Triglycerides (mg/dL)	123.9 ± 12.3	188.4 ± 32.1	0.09
HDL-C (mg/dL)	47.9 ± 3.2	36.7 ± 2.2	<0.01
Amino acids (μmol/L)			
Glycine	205.4 ± 10.0	287.2 ± 18.0	<0.001
Alanine	365.7 ± 9.0	426.5 ± 24.2	0.03
Serine	81.0 ± 4.3	117.0 ± 5.4	<0.001
Proline	167.4 ± 9.0	203.2 ± 11.0	0.02
Valine	215.7 ± 9.5	230.5 ± 11.8	0.34
Isoleucine/leucine	156.3 ± 7.8	178.5 ± 9.7	0.08
Total BCAA	372.0 ± 17	409.0 ± 21	0.2
Isoleucine (by HPLC) ^C	62.2 ± 5.3	59.6 ± 7.0	0.78
Leucine (by HPLC) ^C	137.3 ± 7.7	128.8 ± 11.6	0.55
Methionine	27.8 ± 1.2	23.6 ± 1.3	0.02
Histidine	69.3 ± 2.5	85.2 ± 3.1	<0.001
Phenylalanine	62.2 ± 2.3	64.4 ± 3.5	0.60
Tyrosine	78.5 ± 6.1	67.5 ± 3.3	0.13
Asx	12.5 ± 0.8	28.9 ± 3.8	<0.01
Glx	93.1 ± 6.6	444.8 ± 17.4	<0.0001
Glutamine (new KPD samples) ^D	437.9 ± 16.8	207.2 ± 10.3	0.0001
Glutamate (new KPD samples) ^D	105.9 ± 18.5	192.0 ± 8.0	0.02
Citrulline	31.9 ± 1.7	25.5 ± 1.9	0.02
FFAs (μmol/L)			
Myristic acid (C14)	9.3 ± 1.2	6.8 ± 1.1	0.12
Palmitoleic acid (C16:1)	16.8 ± 2.4	15.1 ± 2.5	0.64
Palmitic acid (C16)	131.8 ± 12.5	111.7 ± 13.6	0.30
α-Linolenic acid (C18:3)	6.7 ± 0.8	5.0 ± 0.7	0.12
Linoleic acid (C18:2)	76.1 ± 7.4	86.5 ± 14.0	0.50
Oleic acid (C18:1)	178.4 ± 18.5	142.4 ± 19.2	0.19
Stearic acid (C18)	44.3 ± 3.7	39.7 ± 4.8	0.45
Molar sum of FFAs	463.4 ± 44.5	407.1 ± 53.9	0.43
Acylcarnitines (μmol/L)			
Acetylcarnitine (C2)	6.86 ± 0.39	5.11 ± 0.29	0.001
Isobutyryl-carnitine (C4)	0.21 ± 0.02	0.29 ± 0.02	0.01
Tiglyl-carnitine (C5:1)	0.05 ± 0.001	0.06 ± 0.001	0.11
Isovaleryl-carnitine			
(2,3 methylbutyryl-carnitine) (C5)	0.16 ± 0.01	0.12 ± 0.01	0.003
β-Hydroxybutyryl-carnitine (C4-OH)	0.02 ± 0.001	0.06 ± 0.01	0.01
Methylmalonyl/succinyl-carnitine (C4-DC)	0.04 ± 0.001	0.02 ± 0.001	<0.001
Glutaryl-carnitine (C5-DC)	0.05 ± 0.001	0.03 ± 0.001	0.001
3-Hydroxyisovaleryl-carnitine (C5-OH)	0.07 ± 0.005	0.05 ± 0.004	0.01

^AIn blood sample obtained 4–12 weeks after recovery from the index episode of DKA. ^BQUICKI = 1/(log fasting glucose + log fasting insulin) (14). Insulin-sensitive persons without metabolic syndrome usually have QUICKI values >0.36 (38). ^CData from a subset of 11 KPD patients and 16 control subjects measured by HPLC. ^DData for KPD from five fresh, new-onset unprovoked A⁻β⁺ KPD patients; these samples were collected and processed exactly as for the control subjects, and glutamine and glutamate in both these KPD samples and the control samples were measured by HPLC.

Absolute synthesis rate (ASR) of glutamate from glutamine:

$$\text{ASR (mmol/L/h)} = \text{ASR} \times \text{Glutamine plasma concentration} \quad \text{Eq. (9)}$$

The rate of formation of $^{13}\text{C}_2$ from $^{13}\text{C}_1$ -glutamine over the 6-h infusion, an index of glutamate dehydrogenase activity, is calculated as follows:

$$^{13}\text{C}_1\text{-glutamine oxidation (mmol/6 h)} = \text{area under the curve of breath } ^{13}\text{C}_2 = \text{AUC}_{0-6 \text{ h}} \text{ of } ^{13}\text{C}_2$$

$$\text{AUC}_{0-6 \text{ h}} \text{ of } ^{13}\text{C}_2 = \text{AUC}[(V_{\text{CO}_2}/0.78) \times \text{IE}_{\text{CO}_2}], \quad \text{Eq. (10)}$$

where $V_{\text{CO}_2}/0.78$ is the production rate of CO_2 , assuming 22% of CO_2 is retained in the bicarbonate pool (22), and IE_{CO_2} is the IE of CO_2 (atom percent excess).

$$\text{Fraction of } ^{13}\text{C}_1\text{-glutamine oxidized} = \frac{\text{AUC}_{0-6 \text{ h}} \text{ } ^{13}\text{C}_2 / \text{total } ^{13}\text{C}_1\text{-glutamine infused}}{\text{AUC}_{0-6 \text{ h}} \text{ } ^{13}\text{C}_2 / \text{total } ^{13}\text{C}_1\text{-glutamine infused}} \quad \text{Eq. (11)}$$

a relative measure of glutamate entry in the TCA cycle at α -ketoglutarate and an estimate of glutaminase plus glutamate dehydrogenase activity.

RESULTS

Metabolomics

Clinical and biochemical parameters. BMI and waist circumference were similar in KPD and control subjects (Table 1). KPD subjects had elevated initial HbA_{1c} ($13.5 \pm 0.5\%$) and fasting plasma glucose levels 4–12 weeks after the index DKA episode. Characteristically, HbA_{1c} was markedly improved 3–6 months after the index DKA (7.2 ± 0.5), when the patients were on low doses of insulin ($N = 13$) or off insulin ($N = 7$). Fasting C-peptide was higher in control subjects. The C-peptide/glucose ratio was one-third of the control level in the KPD group. Fasting insulin levels were not different, and quantitative insulin sensitivity check index (QUICKI), an index of insulin sensitivity, demonstrated similar levels of insulin resistance in the two groups. Triglycerides showed a trend to be higher, and HDL-cholesterol (HDL-C) was $\sim 30\%$ lower in KPD. The mean BOHB level was twice as high in KPD as in control subjects, but the difference did not attain statistical significance due to individual variability. KPD patients had normal fasting metanephrines and cortisol and normal thyroid, renal, and liver functions. The KPD group included 1 white, 7 African American, and 11 Hispanic subjects, whereas the control subjects included 14 white, 4 African American, and no Hispanic subjects; ethnicity was not correlated with any inter- or intragroup differences in metabolite or hormone levels.

Amino acids and related acylcarnitines. “Asx” was 2.3-fold ($P < 0.01$) and “glx” 4.8-fold ($P < 0.0001$) higher in the KPD group (Table 1). Smaller elevations were observed in KPD for glycine (1.4-fold; $P < 0.001$), serine (1.4-fold; $P < 0.001$), alanine (1.2-fold; $P = 0.03$), proline (1.2-fold; $P = 0.02$), and histidine (1.2-fold; $P < 0.001$). Methionine (0.85-fold; $P = 0.02$) and citrulline (0.75-fold; $P = 0.02$) were lower in KPD.

The unusually high levels of glx in KPD suggested partial ex vivo conversion of glutamine to glutamate or pyroglutamine (23–25) in those samples. HPLC also demonstrated very low glutamine and very high glutamate levels in the KPD samples. To avoid alterations of glutamine and glutamate due to collection methods or storage, five additional, newly diagnosed $\text{A}^{-}\beta^{+}$ KPD patients were recruited and their plasma collected using stringent collection and processing methods (26). The mean glutamine concentration in these new KPD samples was $207.20 \pm 10.29 \mu\text{mol/L}$ (0.56-fold less than control subjects; $P = 0.0001$) and the mean glutamate concentration $192.03 \pm 7.98 \mu\text{mol/L}$ (1.75-fold more than control subjects; $P = 0.02$).

Concentrations of total branched chain amino acids (BCAA) were similar in KPD and control subjects, with no significant differences in valine or isoleucine/leucine. Because MS/MS cannot distinguish isoleucine from leucine, HPLC was used to separate them in samples from 11 KPD patients and 16 control subjects. Leucine and isoleucine concentrations were not different between KPD and control subjects (128.8 ± 11.6 vs. 137.3 ± 7.7 and 59.6 ± 7.0 vs. $62.2 \pm 5.3 \mu\text{mol/L}$, respectively; $P = \text{NS}$ for both). This was surprising because fasting plasma concentrations of leucine and isoleucine are usually elevated in diabetic patients with imperfect glycemic control (27–30). Hence, we tracked the catabolic pathways of BCAA through acylcarnitine esters of their distinct ketoacid metabolites (Table 1). Isobutyryl-carnitine (C4-AC), from decarboxylation of the valine ketoacid, was 1.5-fold higher in KPD ($P < 0.01$). In contrast, C5-AC, representing acylcarnitine esters of both isovaleryl-CoA and α -isomethylbutyryl-CoA (from decarboxylation of the leucine and isoleucine ketoacids, respectively), was 1.3-fold lower in KPD ($P < 0.01$), but tiglyl-carnitine (C5:1-AC), an isoleucine-specific catabolite, was 1.2-fold higher in KPD ($P = 0.1$). In sum, these data indicated that the leucine ketoacid metabolite was decreased in KPD patients.

BCAA are deaminated by branch chain aminotransferase (BCAT) to produce KICA from leucine, α -keto- β -methylvaleric acid (KMVA) from isoleucine and α -ketoisovaleric

TABLE 2
Kinetic study: demographic, hormonal, and biochemical data

	Control subjects ($N = 7$)	$\text{A}^{-}\beta^{+}$ KPD ($N = 9$)	P value
Age (years)	43.4 ± 3.1	48.3 ± 4.4	0.37
Sex			
Male	6	6	
Female	1	3	
Weight (kg)	83.5 ± 5.3	87.9 ± 10.9	0.72
BMI (kg/m^2)	28.0 ± 0.9	32.4 ± 2.8	0.16
Fat mass (kg)	26.6 ± 2.3	36.4 ± 6.6	0.19
Initial HbA_{1c} (%)		13.1 ± 0.4	
HbA_{1c} 3 to 4 months later ^A (%)	5.6 ± 0.1	6.5 ± 0.1	<0.001
Fasting glucose (mg/dL)	89 ± 4	93 ± 3	0.44
Fasting C-peptide (ng/mL)	1.57 ± 0.3	1.70 ± 0.4	0.8
Peak C-peptide (ng/mL)	4.39 ± 0.6	3.20 ± 0.5	0.14
Fasting C-peptide/glucose	0.02 ± 0.003	0.02 ± 0.004	0.61
Fasting insulin ($\mu\text{U/mL}$)	14.1 ± 3.2	22.8 ± 3.5	<0.01
QUICKI ^B	0.33 ± 0.3	0.30 ± 0.2	0.05
TSH ($\mu\text{U/mL}$)	2.3 ± 0.5	1.6 ± 0.3	0.28
BUN (mg/dL)	13.3 ± 1.2	16.0 ± 1.5	0.19
Creatinine (mg/dL)	0.97 ± 0.04	0.88 ± 0.09	0.36
ALT (IU/dL)	25 ± 2	47 ± 4	<0.001
AST (IU/dL)	28 ± 4	31 ± 5	0.57

ALT, alanine aminotransferase; BUN, blood urea nitrogen; TSH, thyroid-stimulating hormone. ^AThree to 4 months later applies to KPD patients only. For control subjects, HbA_{1c} was measured once. ^BQUICKI = $1/(\log \text{fasting glucose} + \log \text{fasting insulin})$ (14). Insulin-sensitive persons without metabolic syndrome usually have QUICKI values >0.36 (38).

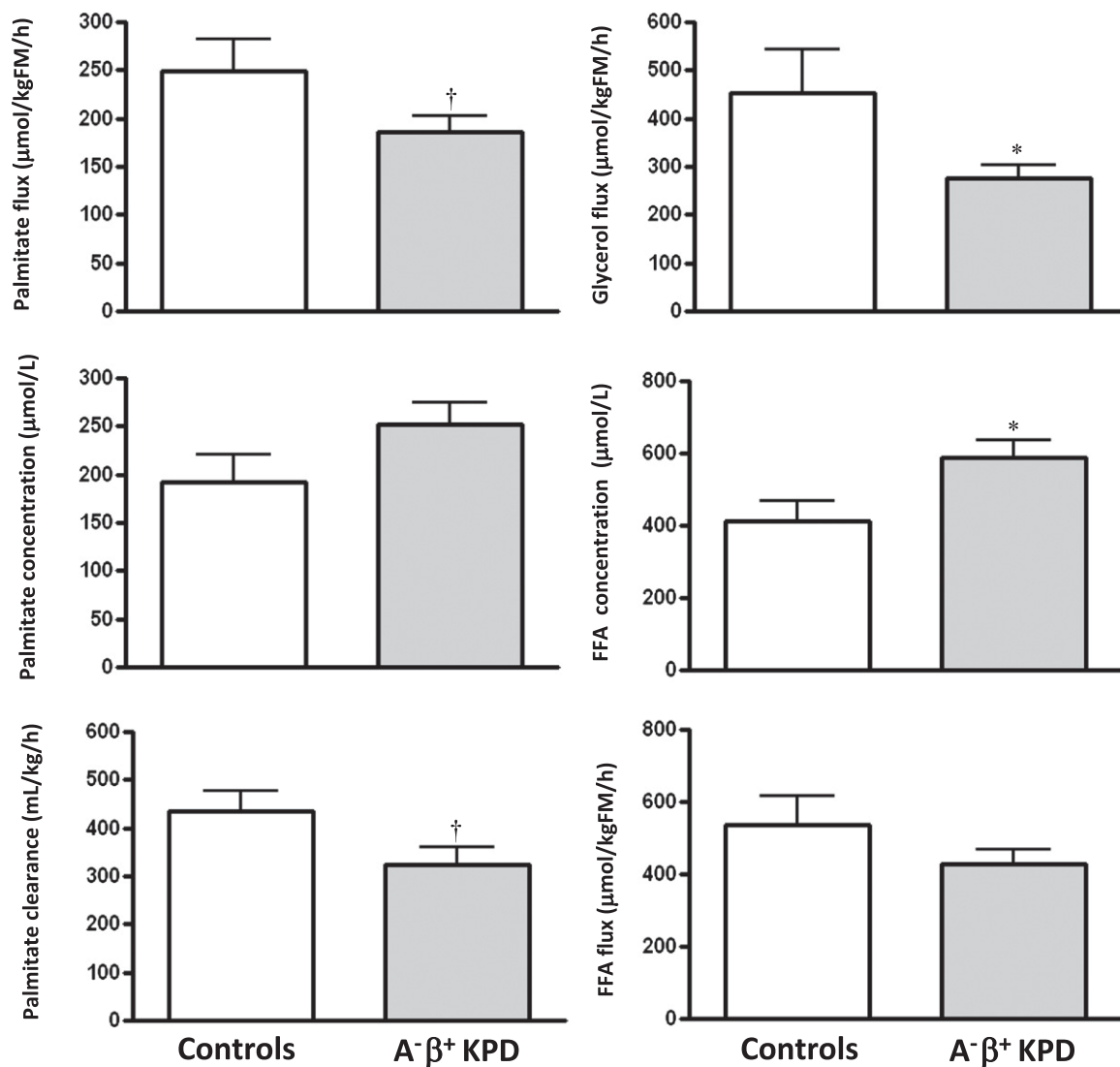


FIG. 1. Lipid kinetics (mean \pm SE) in A $^{-}\beta^{+}$ KPD patients and control subjects. * $P \leq 0.05$; † $P < 0.1$ ($N = 9$ for KPD, $N = 7$ for control subjects).

acid (KIVA) from valine, and the NH_2 group is transferred to α -ketoglutarate to generate glutamate. The ketoacids are processed by branch chain ketoacid dehydrogenase (BCKDH) and subsequently follow distinct pathways to either generate ketone bodies (KICA, KMVA) or enter the TCA cycle for oxidation (KIVA, KMVA). Glutamate is exported from mitochondria with aspartate and the remaining ketoacids. Glutamate, aspartate, KMVA, and KIVA are precursors for gluconeogenesis; in contrast, KICA is a primary amino acid source of ketones. The metabolomic data suggested acceleration of the initial steps of BCAA catabolism in muscle as an explanation for key metabolic signatures in KPD patients: lack of elevated BCAA, low C5-AC, elevated glutamate, and elevated ketones.

TCA/anaplerotic metabolites. Acetylcarnitine (C2, acylcarnitine ester of acetyl CoA) was lower in KPD (1.3-fold; $P = 0.001$), suggesting either decreased production of acetyl CoA or increased shunting of acetyl CoA into oxidative or synthetic pathways (Table 1). β -hydroxybutyryl-carnitine (C4-OH), representing intracellular BOHB, was threefold higher in KPD ($P = 0.01$), suggesting increased ketone synthesis or diminished ketone oxidation. Other short-chain acylcarnitines (C4-DC, C5-DC), which include metabolites

arising distal to α -ketoglutarate in the TCA cycle, such as methylmalonyl/succinyl-carnitine and glutaryl-carnitine, were diminished in KPD.

Fatty acids and ketones. The molar sum of the seven most abundant fatty acids was similar in KPD and control subjects (Table 1). Persons consuming American diets have the following rank order of fasting fatty acid concentrations: oleate $>$ palmitate \geq linoleate (31); this order was preserved in both groups, and levels of palmitate and oleate were similar, making it unlikely that there were group differences in habitual dietary fat composition. These data suggested that the proclivity for ketosis in KPD patients is not due to excessive fatty acid supply.

Kinetics. In the kinetic study cohort, age, weight, and BMI were similar in the two groups (Table 2). HbA_{1c} was very high in the KPD patients at the time of the index DKA; 3 to 4 months later, mean HbA_{1c} and fasting glucose were markedly improved, but still higher than in the control subjects. At that time, fasting and glucagon-stimulated peak C-peptide and C-peptide/glucose ratio were similar in KPD and control subjects. Fasting insulin levels were higher in KPD; however, they were very similar to those of the KPD patients in the metabolomics study (Table 1), and

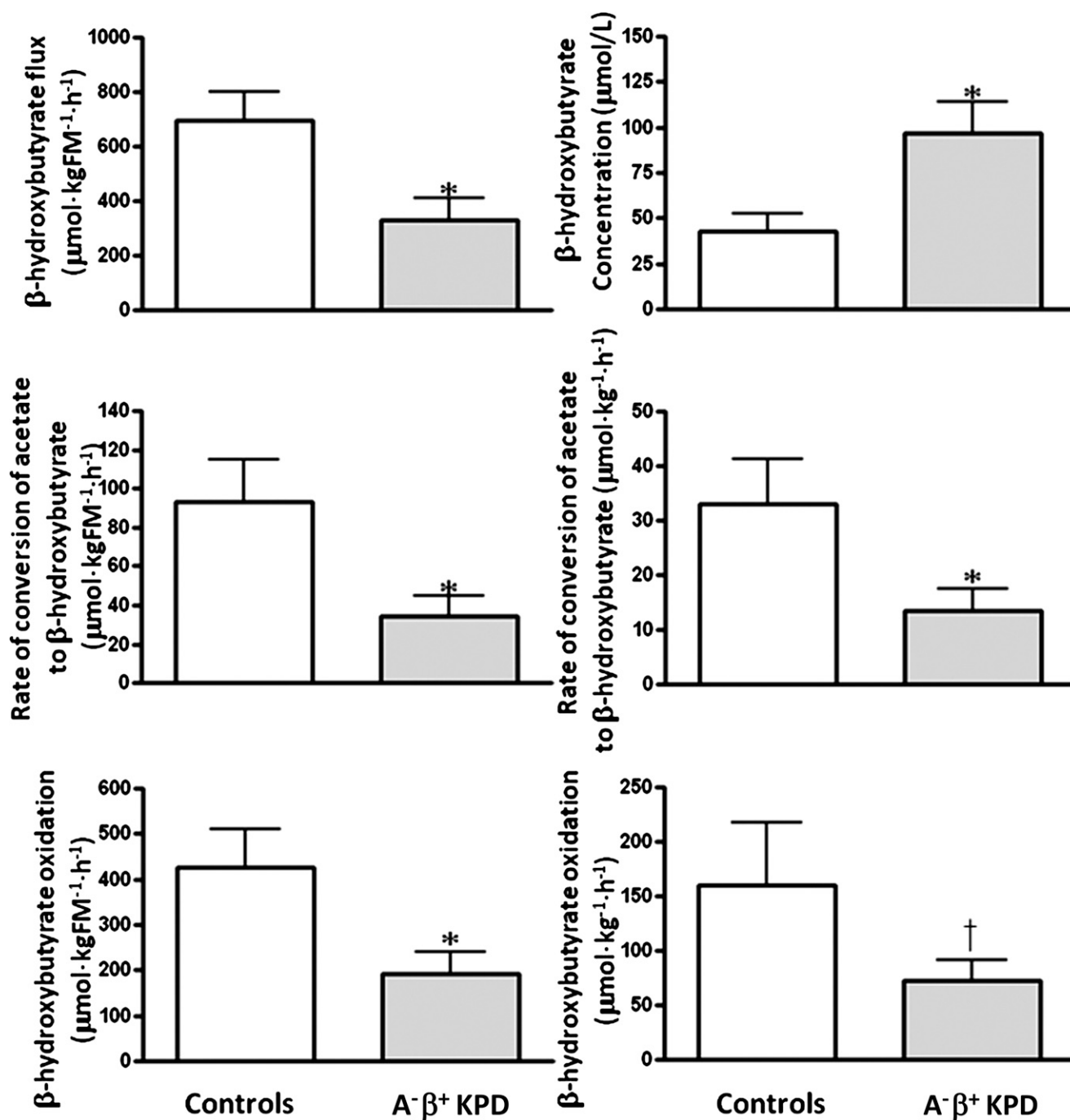


FIG. 2. BOHB concentration, rate of conversion of acetate to BOHB, BOHB flux, and BOHB oxidation (mean \pm SE) in A⁻β⁺ KPD patients and control subjects (for BOHB concentration: $N = 9$ for KPD, $N = 7$ for control subjects; for all other measurements $N = 7$ for KPD, $N = 3$ for control subjects). * $P < 0.05$; † $P = 0.09$.

QUICKI demonstrated a significantly higher degree of insulin resistance in KPD. Thyroid-stimulating hormone, blood urea nitrogen, creatinine, and AST were normal and similar in both groups. Triglycerides (163 ± 9 mg/dL) were elevated, whereas HDL-C (40.6 ± 3.9 mg/dL) was low, and LDL-cholesterol level was 85 ± 9 mg/dL in the KPD group. 1. Fasting rates of FFA release and acetyl CoA flux are similar in KPD and control subjects. BOHB oxidation and fatty acid disposal are slowed, leading to elevated plasma concentrations of BOHB and FFA.

Ra FFA (total FFA flux) was not different, whereas Ra glycerol (index of triglyceride hydrolysis) was significantly

lower, and Ra palmitate (palmitate flux) trended lower in KPD (Fig. 1). Furthermore, Ra acetate (index of whole-body acetyl CoA flux) was similar in KPD and control subjects ($1,344 \pm 260$ vs. $1,570 \pm 141$ $\mu\text{mol}/\text{kgFM}/\text{h}$; $P = 0.50$), and acetate oxidation (breath ¹³CO₂ liberated by isocitrate dehydrogenase activity, reflecting acetyl CoA flux through the TCA cycle) was also similar (861 ± 175 vs. $1,007 \pm 87$ $\mu\text{mol}/\text{kgFM}/\text{h}$; $P = 0.49$). Despite the similar FFA flux, plasma concentration of FFA was higher in KPD (587 ± 51 vs. 412 ± 8 $\mu\text{mol}/\text{L}$; $P = 0.04$) (Fig. 1), suggesting slower FFA disposal (corroborated by the slower palmitate clearance). Plasma concentration of BOHB was

also higher in the KPD patients (97 ± 17 vs. 43 ± 10 $\mu\text{mol/L}$; $P = 0.02$) in the face of slower conversion of acetyl CoA to BOHB (Fig. 2). Collectively, these findings indicated defective BOHB and fatty acid disposal, which, after a 10–14-h fast, is predominantly oxidative. To test BOHB oxidation directly, protocol 4 was performed in three control subjects and seven KPD patients. KPD had slower BOHB flux (330 ± 80 vs. 696 ± 103 $\mu\text{mol/kgFFM/h}$; $P = 0.03$) but also slower oxidative BOHB disposal (191 ± 47 vs. 427 ± 84 $\mu\text{mol/kgFFM/h}$; $P = 0.03$), a combination that would increase BOHB concentration. (Of note, plasma BOHB enrichment was used in this study as a proxy for intracellular acetate or acetyl CoA enrichment; in reality, it is acetyl CoA that is oxidized. The IE of the acetyl CoA would be lower than the plasma BOHB enrichment, because there are additional sources of unlabeled acetyl CoA in the intracellular pool. Because the more highly enriched BOHB is the denominator used in the calculations, the actual oxidation rate of BOHB [which must first be converted to acetyl CoA to be oxidized via intermediates in the TCA cycle] is probably underestimated in all subjects.)

2. Oxidative decarboxylation of leucine is accelerated in KPD.

There was no difference between KPD and control subjects in leucine flux and a trend toward higher valine flux in KPD (Fig. 3). The rate of oxidative decarboxylation, or removal of the #1 carbon of leucine by BCKDH, showed a strong trend to be faster in KPD (60.0 ± 2.8 vs. 51.7 ± 2.9 $\mu\text{mol/kgFFM/h}$; $P = 0.06$). Increased BCKDH activity requires increased flux through the earlier BCAT-catalyzed step that drives transfer of NH_2 from leucine to α -ketoglutarate to generate glutamate (32). Unless matched by acceleration of the opposing reaction that oxidatively deaminates glutamate to α -ketoglutarate, this would promote accumulation of glutamate.

3. Conversion of glutamine to glutamate is accelerated in KPD, without a parallel increase in glutamate carbon oxidation.

There was no group difference in glutamine flux, but plasma glutamine concentration trended lower in KPD (557 ± 29 vs. 655 ± 36 $\mu\text{mol/L}$; $P = 0.06$) (Fig. 4A). The rate of glutamine carbon transfer to glutamate was faster in KPD by several measures: slope of change, absolute synthesis rate of glutamate from glutamine (Fig. 4A), and fractional synthesis rate of glutamate from glutamine (Fig. 4B). However, the rate of oxidation of the same glutamate carbon in the TCA cycle was not different between the groups (Fig. 4B). Thus, increased glutamate production from glutamine in KPD is not matched by a parallel increase in glutamate carbon anaplerosis into the TCA cycle, as predicted from the results of the leucine infusion study.

4. Transfer of amide nitrogen from glutamine to citrulline is slower in KPD.

Citrulline flux was slower in KPD than in control subjects (Fig. 5), with a trend toward slower transfer of glutamine amide nitrogen to ornithine (7.8 ± 0.4 vs. 8.6 ± 0.3 $\mu\text{mol/kgFFM/h}$; $P = 0.1$) for citrulline synthesis.

DISCUSSION

In this study, the pathophysiology of $\text{A}^{-}\beta^{+}$ KPD was investigated comprehensively using a two-step discovery method. First, fasting plasma metabolomics compared KPD patients to nondiabetic obese subjects. Hypotheses generated from key differences were tested by kinetic

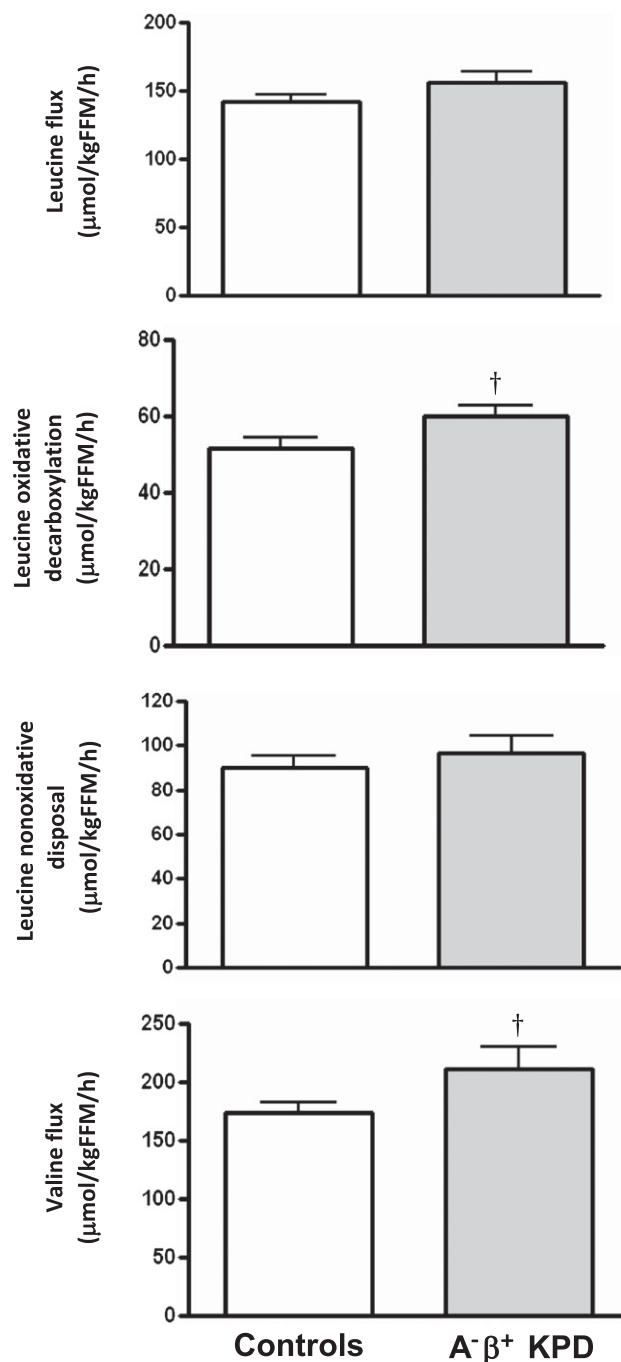


FIG. 3. Leucine flux, oxidative decarboxylation, and nonoxidative disposal and valine flux (mean \pm SE) in $\text{A}^{-}\beta^{+}$ KPD patients and control subjects. † $P = 0.06$ ($N = 9$ for KPD, $N = 7$ for control subjects).

tracer studies targeting the suspected metabolic pathways in a fresh cohort of patients and control subjects.

The metabolomic analysis revealed signals of altered BCAA catabolism in KPD associated with changes in glutamine/glutamate. We hypothesized that the lack of elevated leucine in KPD was due to accelerated catabolism of this amino acid, indicated by decreased C5-AC and elevated glutamate (33,34). Evidence that accelerated leucine catabolism extended beyond isovaleryl CoA to β -methylcrotonyl CoA and ketogenesis was provided by the lower level of 3-hydroxyisovaleryl-carnitine (C5-OH). Concomitantly,

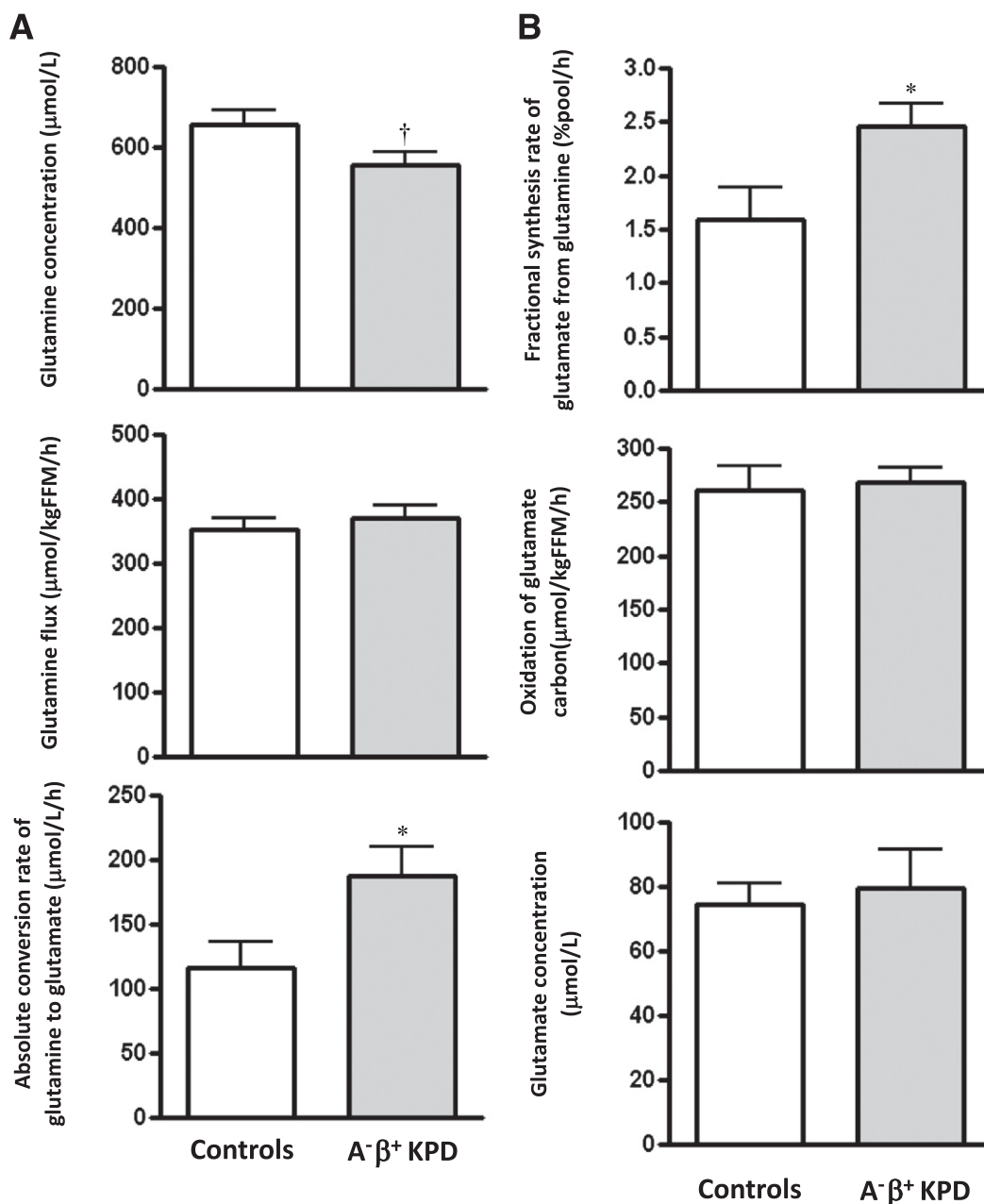


FIG. 4. *A*: Glutamine flux, glutamine plasma concentration, and absolute conversion rate of glutamine to glutamate (mean \pm SE) in A⁻β⁺ KPD patients and control subjects ($N = 9$ for KPD, $N = 7$ for control subjects). *B*: Fractional synthesis rate of glutamate from glutamine, oxidation of glutamate carbon (derived from glutamine), and glutamate plasma concentration (mean \pm SE) in A⁻β⁺ KPD patients and control subjects. * $P < 0.05$; † $P = 0.06$ ($N = 9$ for KPD, $N = 7$ for control subjects).

glutamine was 50% lower, whereas glutamate was 175% higher, in KPD. Glutamine and glutamate are nitrogen sinks for catabolism of other amino acids, including BCAA, in the fasted state. Elevated glutamate and decreased glutamine levels could reflect absence of upregulation of glutamate oxidation rates in KPD subjects in the face of faster conversion of glutamine to glutamate and accelerated leucine deamidation.

Changes in small-chain acylcarnitines reflecting TCA cycle intermediates and anaplerosis broadened the pathophysiologic hypothesis. Acetylcarnitine was significantly lower in KPD, suggesting decreased production or increased consumption of acetyl CoA. Acylcarnitines that include glutaryl CoA and succinyl CoA were lower and

β-hydroxybutyryl-carnitine was threefold higher in KPD, suggesting diversion of acetyl CoA disposal toward ketogenesis. Finally, fasting FFA levels and composition were similar in KPD and control subjects, suggesting that excessive fatty acid flux from lipolysis is not the driver of ketogenesis in KPD.

In sum, the metabolomic data suggested that patients with unprovoked A⁻β⁺ KPD have accelerated leucine catabolism toward ketogenesis. This would expand the nitrogen sinks of transamination reactions, resulting in elevated levels of glutamate and aspartate. The data also indicated that KPD patients have defects in transferring carbon from glutamine/glutamate to the TCA cycle and nitrogen from glutamine/glutamate to the urea cycle.

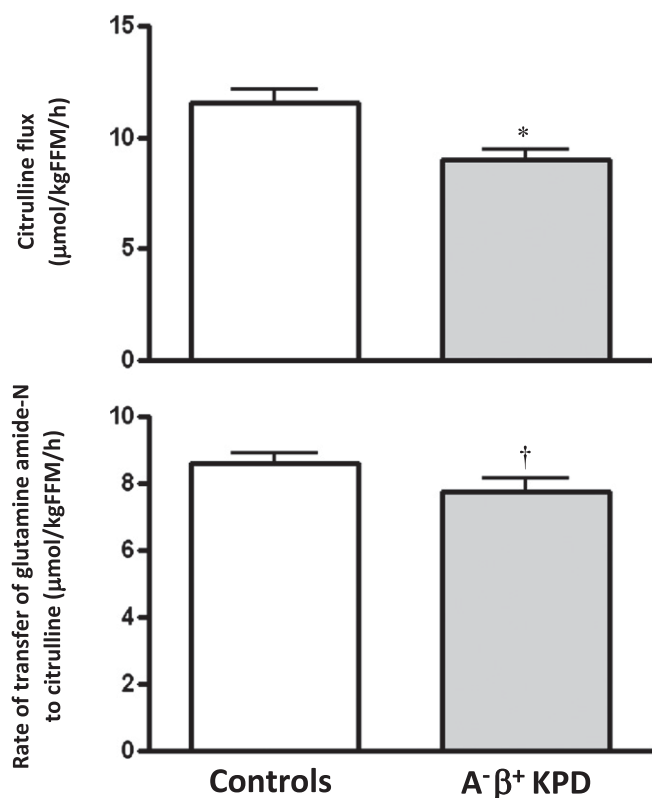


FIG. 5. Citrulline flux and rate of transfer of glutamine amide-N to citrulline (mean ± SE) in A⁻β⁺ KPD patients and control subjects. **P* < 0.05; †*P* = 0.10 (*N* = 9 for KPD, *N* = 7 for control subjects).

The results of the kinetic studies confirmed the hypothesis and revealed also that KPD patients have altered ketone oxidation. Clinically stable KPD patients with excellent glycemic control have elevated plasma BOHB. The cause is not excessive fatty acid-derived ketone production—the conversion of acetyl CoA to BOHB is slower, and rates of acetyl CoA flux and isocitrate decarboxylation are unaltered. However, the rate of ketone oxidation is significantly slowed in KPD, leading to elevated concentrations of BOHB and its intracellular metabolites, and this likely plays a prominent role in the most unique characteristic of the phenotype, proclivity for ketosis. Fatty acid disposal is also impaired.

Unable to maximize rates of oxidation of fat-derived sources for energy, KPD patients after an overnight fast draw upon amino acids for energy. There is increased flux through the leucine catabolic pathway toward ketone production. Acceleration of leucine catabolism also leads, through reductive deamination of α-ketoglutarate, to glutamate accumulation (exacerbated by increased conversion from glutamine) and blunted glucose carbon anaplerosis in the TCA cycle as manifested by an unchanged rate of glutamate carbon oxidation. A similar cascade occurs in McArdle syndrome, in which accelerated BCAA catabolism eventually reduces flux into the TCA cycle through increased conversion of α-ketoglutarate to glutamate (35).

Peripheral oxidation of ketone bodies is a TCA cycle-dependent process; in this regard, an apparent conflict arises between the finding of slowed BOHB oxidation in KPD and the finding that there is no difference in the rate of oxidation in the TCA cycle when the groups are challenged with a similar flux of oxidative substrate

(¹³C₁-acetate). This apparent paradox may be explained because our measurements specifically demonstrate that KPD show no defect in the rate of removal of CO₂ from isocitrate (at the step of isocitrate dehydrogenase) in the TCA cycle, and this leaves open the possibility of kinetic defects distal to that step in the TCA cycle and therefore in the rates at which reduced energy intermediates are delivered for oxidative phosphorylation. The data suggest that there may be such a kinetic defect at the level of α-ketoglutarate dehydrogenase associated with more rapid decarboxylation of leucine, as evidenced by the accumulation of glutamate and reduced levels of acylcarnitines of TCA intermediates beyond that step.

This study combines for the first time an unbiased metabolomics approach and a targeted kinetics approach to specify the pathophysiology of a novel diabetic syndrome (Fig. 6). Umpierrez et al. (36) previously explored the pathophysiology of ketosis-prone type 2 diabetes, a condition identical to unprovoked A⁻β⁺ KPD. They reported no ketosis or β-cell decompensation following prolonged infusion of fatty acids, supporting the concept that proneness to ketosis in KPD is not due to excessive fatty acid flux to the liver.

Defective oxidation of ketones and accelerated leucine catabolism are key defects of fasting energy metabolism that underlie the distinctive syndrome of unprovoked A⁻β⁺ KPD. The findings indicate the need to investigate mitochondrial function and BCAT and BCKDH regulation in the skeletal muscle of KPD patients. These defects are associated with pronounced changes in glutamine/glutamate metabolism; interestingly, elevated glutamate predicted type 1 diabetes in a longitudinal metabolomics study (37). Clinically and metabolically, patients with A⁻β⁺ KPD manifest features of both type 1 and type 2 diabetes. The present data explain how overweight patients with a type 2 diabetes phenotype and adequate β-cell reserve are prone to developing unprovoked ketoacidosis. The coupled metabolomics-kinetics approach should be useful in elucidating the pathophysiology of other phenotypes of diabetes.

ACKNOWLEDGMENTS

This study was supported by National Institutes of Health (NIH) R21-DK-082827 (to A.B.), the Diabetes and Endocrinology Research Center (P30-DK-079638) at Baylor College of Medicine, NIH RO1-DK-056689 (to F.J.), funds from the U.S. Department of Agriculture, Agricultural Research Service under Cooperative Agreement Number 58-6250-6001, and NIH PO1-DK-58398 (to C.B.N.).

No potential conflicts of interest relevant to this article were reported.

S.G.P. and F.J. helped to design the kinetic studies, analyzed data, and edited the manuscript. J.W.H. performed mass spectrometric analyses and analyzed data. I.C. recruited subjects and implemented the stable isotope protocols. J.R.B. and R.D.S. performed metabolomic analyses and reviewed the manuscript. D.I. performed biochemical assays. R.N. and K.O. maintained clinical care of the study subjects and edited the manuscript. C.S.H. performed autoantibody testing of the study subjects and reviewed the manuscript. C.B.N. helped with study design, supervised the metabolomic analyses, and edited the manuscript. A.B. designed and obtained funding for the study, implemented the kinetic protocols, analyzed data, and wrote the manuscript. A.B. is the guarantor of

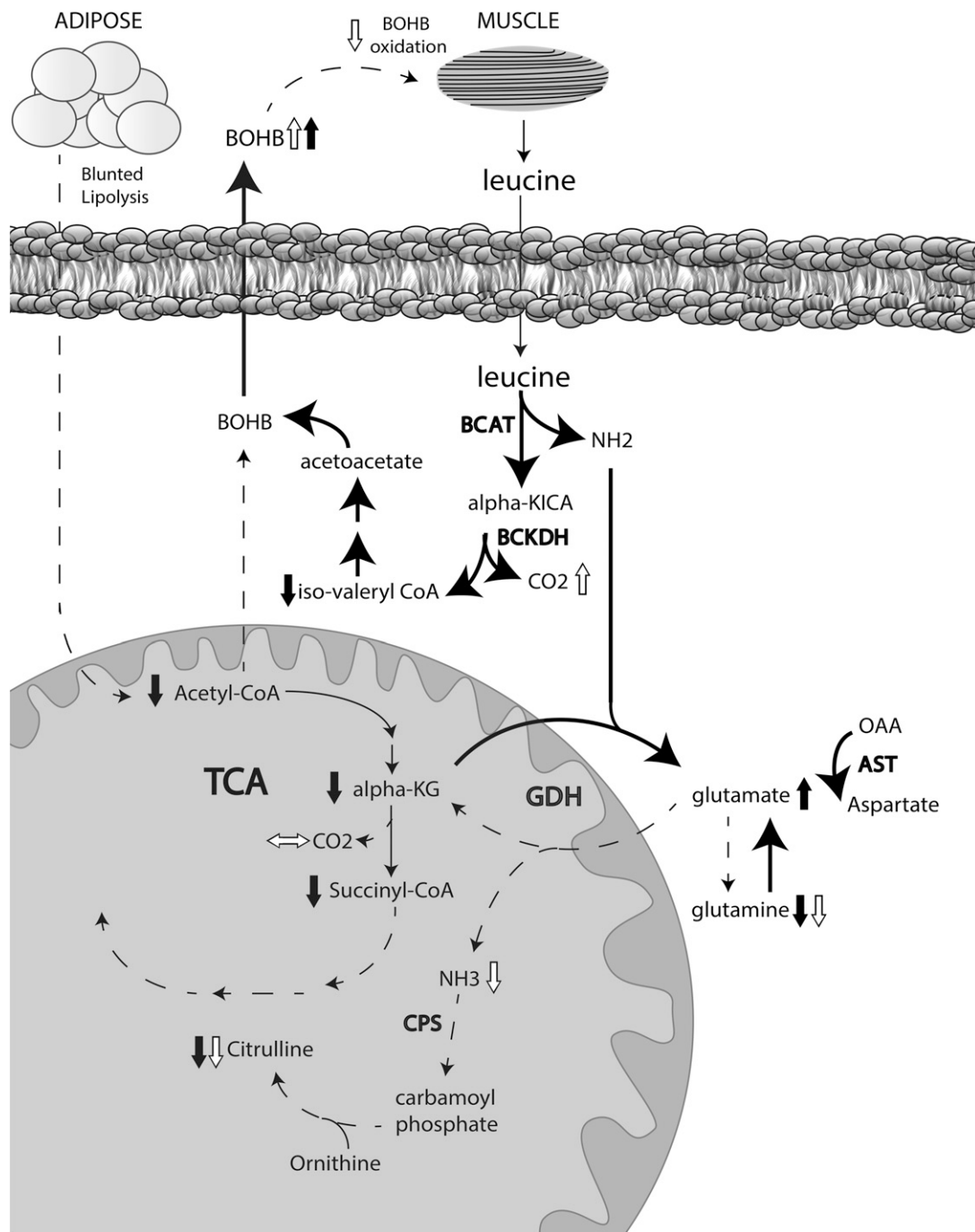


FIG. 6. Schematic representation of metabolic defects in KPD as revealed by a combination of metabolomics and kinetics. Short black arrows represent increase or decrease in a metabolite measured in the metabolomics survey, whereas short white arrows represent increase, decrease, or no change in a metabolite measured in the kinetic studies. Lipid bilayer indicates the boundary of a liver cell. Dashed long arrows indicate decreased flux, and solid long arrows indicate increased flux. See text for details. alpha-KG, alpha-ketoglutarate; CPS, carbamoyl phosphate synthetase; GDH, glutamate dehydrogenase.

this work and, as such, had full access to all the data in the study and takes responsibility for the integrity of the data and the accuracy of the data analysis.

Parts of this study were presented in poster form at the 71st Scientific Sessions of the American Diabetes Association, San Diego, California, 24–28 June 2011.

The authors thank Elizabeth Fraser, Vy Pham, and Toni Oplt (all from Baylor College of Medicine) for technical assistance; Resa Labbe-Morris, RN, and the nursing staff of

the Baylor College of Medicine General Clinical Research Center for meticulous attention to protocol and care of the study subjects; Varsha Patel, RPh, and the Investigational Pharmacy (The Methodist Hospital Research Institute, Houston, TX) for stable isotope preparation; Drs. Heinrich Taegtmeier (University of Texas Health Sciences Center, Houston, TX), William Mitch, and Arun Sreekumar (both from Baylor College of Medicine) for helpful discussions; and all of the study subjects.

REFERENCES

- Maldonado M, Hampe CS, Gaur LK, et al. Ketosis-prone diabetes: dissection of a heterogeneous syndrome using an immunogenetic and beta-cell functional classification, prospective analysis, and clinical outcomes. *J Clin Endocrinol Metab* 2003;88:5090–5098
- Kitabchi AE. Ketosis-prone diabetes—a new subgroup of patients with atypical type 1 and type 2 diabetes? *J Clin Endocrinol Metab* 2003;88:5087–5089
- Mauvais-Jarvis F, Sobngwi E, Porcher R, et al. Ketosis-prone type 2 diabetes in patients of sub-Saharan African origin: clinical pathophysiology and natural history of beta-cell dysfunction and insulin resistance. *Diabetes* 2004;53:645–653
- Umpierrez GE, Smiley D, Kitabchi AE. Narrative review: ketosis-prone type 2 diabetes mellitus. *Ann Intern Med* 2006;144:350–357
- Balasubramanyam A, Nalini R, Hampe CS, Maldonado M. Syndromes of ketosis-prone diabetes mellitus. *Endocr Rev* 2008;29:292–302
- Balasubramanyam A, Garza G, Rodriguez L, et al. Accuracy and predictive value of classification schemes for ketosis-prone diabetes. *Diabetes Care* 2006;29:2575–2579
- Banerji MA, Dham S. A comparison of classification schemes for ketosis-prone diabetes. *Nat Clin Pract Endocrinol Metab* 2007;3:506–507
- Umpierrez GE, Casals MM, Gebhart SP, Mixon PS, Clark WS, Phillips LS. Diabetic ketoacidosis in obese African-Americans. *Diabetes* 1995;44:790–795
- Maldonado MR, Otiniano ME, Cheema F, Rodriguez L, Balasubramanyam A. Factors associated with insulin discontinuation in subjects with ketosis-prone diabetes but preserved beta-cell function. *Diabet Med* 2005;22:1744–1750
- Nalini R, Ozer K, Maldonado M, et al. Presence or absence of a known diabetic ketoacidosis precipitant defines distinct syndromes of “A-β+” ketosis-prone diabetes based on long-term β-cell function, human leukocyte antigen class II alleles, and sex predilection. *Metabolism* 2010;59:1448–1455
- Nalini R, Gaur LK, Maldonado M, et al. HLA class II alleles specify phenotypes of ketosis-prone diabetes. *Diabetes Care* 2008;31:1195–1200
- Rasouli N, Elbein SC. Improved glycemic control in subjects with atypical diabetes results from restored insulin secretion, but not improved insulin sensitivity. *J Clin Endocrinol Metab* 2004;89:6331–6335
- Newgard CB, An J, Bain JR, et al. A branched-chain amino acid-related metabolic signature that differentiates obese and lean humans and contributes to insulin resistance. *Cell Metab* 2009;9:311–326
- Chen H, Sullivan G, Quon MJ. Assessing the predictive accuracy of QUICKI as a surrogate index for insulin sensitivity using a calibration model. *Diabetes* 2005;54:1914–1925
- Ho DE, Imai K, King G, Stuart EA. MatchIt: Nonparametric preprocessing for parametric causal inference [Internet], 2011. Vol. 42, Issue 8. *Journal of Statistical Software*. Available from <http://www.jstatsoft.org/v42/i08>
- Duarte NL, Wang XL, Wilcken DE. Effects of anticoagulant and time of plasma separation on measurement of homocysteine. *Clin Chem* 2002;48:665–668
- Hachey DL, Patterson BW, Reeds PJ, Elsas LJ. Isotopic determination of organic keto acid pentafluorobenzyl esters in biological fluids by negative chemical ionization gas chromatography/mass spectrometry. *Anal Chem* 1991;63:919–923
- Mohammad MA, Sunehag AL, Rodriguez LA, Haymond MW. Galactose promotes fat mobilization in obese lactating and nonlactating women. *Am J Clin Nutr* 2011;93:374–381
- Kao CC, Bandi V, Guntupalli KK, Wu M, Castillo L, Jahoor F. Arginine, citrulline and nitric oxide metabolism in sepsis. *Clin Sci (Lond)* 2009;117:23–30
- Frayn KN. Calculation of substrate oxidation rates in vivo from gaseous exchange. *J Appl Physiol* 1983;55:628–634
- Sidossis LS, Coggan AR, Gastaldelli A, Wolfe RR. A new correction factor for use in tracer estimations of plasma fatty acid oxidation. *Am J Physiol* 1995;269:E649–E656
- Wolfe RR, Jahoor F. Recovery of labeled CO₂ during the infusion of C-1- vs C-2-labeled acetate: implications for tracer studies of substrate oxidation. *Am J Clin Nutr* 1990;51:248–252
- Schaefer A, Piquard F, Haberey P. Plasma amino-acids analysis: effects of delayed samples preparation and of storage. *Clin Chim Acta* 1987;164:163–169
- Reichert MC. Innovations in sterilization technology for instrument processing. *Med Instrum* 1983;17:89–90
- Ukida M, Schäfer K, Bode JC. Effect of storage at 20° C on the concentration of amino acids in plasma. *J Clin Chem Clin Biochem* 1981;19:1193–1195
- Scriver CR, Lamm P, Clow CL. Plasma amino acids: screening, quantitation, and interpretation. *Am J Clin Nutr* 1971;24:876–890
- Felig P, Marliss E, Ohman JL, Cahill CF Jr. Plasma amino acid levels in diabetic ketoacidosis. *Diabetes* 1970;19:727–728
- Wahren J, Felig P, Cerasi E, Luft R. Splanchnic and peripheral glucose and amino acid metabolism in diabetes mellitus. *J Clin Invest* 1972;51:1870–1878
- Carlsten A, Hallgren B, Jagenburg R, Svanborg A, Werkö L. Amino acids and free fatty acids in plasma in diabetes. I. The effect of insulin on the arterial levels. *Acta Med Scand* 1966;179:361–370
- Nair KS, Garrow JS, Ford C, Mahler RF, Halliday D. Effect of poor diabetic control and obesity on whole body protein metabolism in man. *Diabetologia* 1983;25:400–403
- Stefan N, Wahl HG, Fritsche A, Häring H, Stumvoll M. Effect of the pattern of elevated free fatty acids on insulin sensitivity and insulin secretion in healthy humans. *Horm Metab Res* 2001;33:432–438
- Hutson SM. The case for regulating indispensable amino acid metabolism: the branched-chain alpha-keto acid dehydrogenase kinase-knockout mouse. *Biochem J* 2006;400:e1–e3
- Darmaun D, Déchelotte P. Role of leucine as a precursor of glutamine alpha-amino nitrogen in vivo in humans. *Am J Physiol* 1991;260:E326–E329
- Darmaun D, Matthews DE, Bier DM. Physiological hypercortisolemia increases proteolysis, glutamine, and alanine production. *Am J Physiol* 1988;255:E366–E373
- Wagenmakers AJ, Coakley JH, Edwards RH. Metabolism of branched-chain amino acids and ammonia during exercise: clues from McArdle's disease. *Int J Sports Med* 1990;11(Suppl. 2):S101–S113
- Umpierrez GE, Smiley D, Robalino G, Peng L, Gosmanov AR, Kitabchi AE. Lack of lipotoxicity effect on beta-cell dysfunction in ketosis-prone type 2 diabetes. *Diabetes Care* 2010;33:626–631
- Oresic M, Simell S, Sysi-Aho M, et al. Dysregulation of lipid and amino acid metabolism precedes islet autoimmunity in children who later progress to type 1 diabetes. *J Exp Med* 2008;205:2975–2984
- Hřebíček J, Janout V, Malincíková J, Horáková D, Cízek L. Detection of insulin resistance by simple quantitative insulin sensitivity check index QUICKI for epidemiological assessment and prevention. *J Clin Endocrinol Metab* 2002;87:144–147